JEE Journal of Ecological Engineering

Journal of Ecological Engineering 2023, 24(3), 287–303
https://doi.org/10.12911/22998993/158563
ISSN 2299–8993, License CC-BY 4.0

Received: 2022.12.01
Accepted: 2023.01.05
Published: 2023.01.15

Effect of Magnetite Oxide Nanoparticles and Tungsten Oxide Nanoparticles on Phosphate Removal from Aqueous Solutions

Amro El-Baz[1*], Mona Mokhtar[2], Ahmed Abdo[1]

[1] Environmental Engineering Department, Faculty of Engineering, Zagazig University, Zagazig 44519, Egypt

[2] Demonstrator at Civil Engineering Department, Mansoura College Academy, Damietta High Way Mansoura, Egypt

* Corresponding author's e-mail: amroaelbaz@gmail.com

ABSTRACT

Phosphate (P) removal from aqueous solutions were studied by a new mineral adsorbent, tungsten (VI) oxide (WO_3) nanoparticles (NPs), which has not been the subject of much research in the field of removing P contaminants from agricultural wastewater. In this paper, P was removed from aqueous solutions by a new mineral adsorbent, WO_3 NPs and it was compared with magnetite (iron IV) oxide (Fe_3O_4) nanoparticles (NPs) under the same ambient operating conditions i.e., The influence of the dosage of adsorbents, initial P concentration, contact time, pH and temperature. The values that achieved the best removal were recorded. It was concluded that the best limits for pH were at 2–3, contact time at 40 minutes, temperature at 45 °C and adsorbent dose at 1.0 g/L. Best results of the variables were applied on samples of real agricultural wastewater, which achieved removal ratio of 77.3% and 75.42% for Fe_3O_4 and WO_3 NPs, respectively. SEM, EDX and FTIR images and analyses were conducted to describe the characteristics of nano-adsorbents used before and after P adsorption in aqueous solutions. The P adsorption kinetics for aqueous solutions were examined by fitting results of the experiment to both the first & second pseudo-kinetically models. The outcome indicated that kinematic data fit better with pseudo-second-order kinetic models. Moreover, the information captured from equilibrium adsorption was analyzed using isothermal methods (by Langmuir & Freundlich Forms). Their results showed that the Freundlich form is considered more suitable than Langmuir form in analyzing the biosorption of P ions. The thermodynamic demeanor of P adsorption by Fe_3O_4 and WO_3 NPs was analyzed and evaluated, and the thermodynamic data analyses confirmed the process of P adsorption was spontaneous. The $\Delta G°$ value was negative, while $\Delta H°$ and $\Delta S°$ values found to be positive, which means that the adsorption of P was a spontaneous, random and endothermic operation. In general, Fe_3O_4 and WO_3 nanoparticles had a high efficiency in removing phosphate from water. In addition, WO_3 NPs has been identified as one of the most promising adsorbents due to its rapid and effective adsorption of pollutants.

Keywords: phosphate removal, nanoparticles, Fe_3O_4 NPs, WO_3 NPs, adsorption, desorption.

INTRODUCTION

The water is primary source of survival for both humans and all living things. Therefore, water quality is a major factor for the general health of humans and living and aquatic organisms. Despite that, some characteristics of natural water have been changed due to wrong methods used to dispose of human waste and organic or inorganic pollutants and dumping them continuously into the water stream (Pica, 2021). By 2025, two-thirds of the world's population could face water deficiency and it is worth noting that Egypt is one of the countries facing the risks of water scarcity because of the continuous growth in population while the water resources are limited. As the continuous population increase with agricultural and industrial development, large quantities of untreated municipal waste and industrial wastewater are disposed of in the Nile River or

in the agricultural drains, which makes this water unsuitable for human use and other living organisms, since it contains of dangerous bacteria and viruses and organic and inorganic compounds that threaten public health, as indicated by Gomaah et al. (2021). Therefore, the increasing need for clean water at low prices is one of the most human goals necessary for the continuation of human life and all other living creatures. The use of non-conventional water sources and the reuse and treatment of industrial and agricultural wastewater has become a necessity to reduce the consumption of natural water and highlight its importance. It should be mentioned that the kind and concentration of contaminants affect natural running water in different ways.

One such contaminant that negatively affects water quality and the living organisms in it is phosphate (P), which is a necessary nutrient in the natural water environment. The element is often found in low quantities. P quantity in water can increase due to man-made sources of residues and waste such as detergents, fertilizers, pesticides, additives, improper disposal of domestic sewage and industrial wastewater, agricultural runoff from crop irrigation water, and wastewater from animal fattening fields (Segun & Olalekan, 2021). All of these can lead to a rise in P concentration, which causes a change in environment and water quality and leads to the damage of the natural food chain of aquatic organisms through a lack of the quantity of oxygen dissolved in water necessary for support the survival and growth of living organisms, as this may lead to end its life, due to lack of oxygen due to the growth of harmful aquatic algae and aquatic plants from eutrophication (Chen et al., 2013).

The Environmental Protection Agency (EPA), states that the overall amount of P in water streams should not be more than 0.05 mg/L (Khodadadi et al., 2017). Taha et al. (2004) mentioned that the P concentration in Egypt in irrigation canals is between 7 and 10 mg/L, while in drainage channels is from 2 to 12 mg/L.

Most traditional treatment methods such as biological treatment, chemical oxidation, chemical precipitation, physicochemical, and others are generally effective, but often require high cost, labor and energy, and sometimes do not reach the required efficiency. This is why the ability to reduce pollutants from water efficiently, effectively and at low cost and bring them to safe levels is so important, so advanced technologies have been resorted to produce clean water with high efficiency and at low cost that is safe for humans or the environment (Adeleye et al., 2016). Therefore, the usage of affordable sorbents has received a lot of attention in recent years, where cost has been considered an important criterion in choosing the technology to absorb pollutants such as P, whether synthetic sorbents or natural sorbents (Mishra et al., 2010). Therefore, in this regard, nanotechnologies can play an important role because of its unique and distinctive properties. Nanomaterials can offer a wide range of applications because they have a very large adsorption capacity; therefore, they have recently been widely applied in polluted water purification and treatment processes. Recently, a lot of studies targeting removal of different specific pollutants in water by nanomaterials have been done, because it has often been proven to be highly efficient and inexpensive, as pointed out (Adeleye et al., 2016). Metal oxides, such as Fe_3O_4, ZrO_2 and CuO, has been widely explored to remove P as they exhibit substantial adsorption to it (Chen et al., 2015). The advantages of using adsorption with metallic nanomaterials are their absorbable nature, ability to regeneration of sorbents used in many applications (through their adsorption property), flexibility in design, operation and economic recovery of P (Suhas et al., 2016). It should be mentioned that using nanotechnology in natural treatment of water and sewage not only indicates its ability to overcome various challenges associated with the recognized traditional technology, but also refers to the exploration of a modern and distinct technology for wastewater treatment and reuse, taking into account the economic aspects and international water quality standards to achieve the highest effectiveness and efficiency at the lowest cost (Adeleye et al., 2016).

Among the used metal oxide nanoparticles, tungsten oxide (WO_3) particles matter has been highly studied for its effective properties in removing contaminants from water. In contrast, despite its high pollutant removal properties, its potential for adsorption organic compounds such as P has not been adequately studied yet (Singh & Madras, 2013). Moreover, among the afore-mentioned metallic nanomaterials, Fe_3O_4 is one of the classic, very effective nanoparticles that are used on a huge and large scale in wastewater treatment (Panneerselvam et al., 2011) as well as absorption of P, organic pollutants and other pollutants that affect the nature and water quality. That is

why a great deal of attention was devoted to Fe_3O_4 due to its excellent stability, constant availability, depressed cost, high efficiency in removing P, non-toxicity and excellent insulating properties. Therefore, the goal of this study was to assess NPs potential as a modern and reasonably cost technology to remove ions of P from aqueous solutions. Two NPs materials were used in this study, Fe_3O_4 and WO_3 to remove P from aqueous solutions. The current work was conducted with the aim of: examining the performance and effect of Fe_3O_4 and WO_3 in removing P ions from water solution; studying the influence of operational factors on the efficiency for adsorption, such as: dosage of adsorbents, initial concentration of P, retention period, pH and temperature; comparing adsorption capacity for the two tested NPs materials to know the efficiency of each of them in removing P from water; investigating the use of Langmuir and Freundlich Isotherms and adsorption thermodynamics; evaluating of study the influence of kinetics on biosorption; studying the biosorption properties of them by Fourier transform infrared (FT-IR) spectra and examining its structure using scanning electron microscopy (SEM) and Energy Disperse X-ray (EDX). Optimal operational parameters have been applied to agricultural wastewater using Fe_3O_4 NP and WO_3 NP.

MATERIAL AND METHODS

Chemical materials

Two NPs materials were used in the current study, Fe_3O_4 and WO_3 to remove P from aqueous solutions. The used magnetite (Iron (IV) Oxide Nanoparticles) (Fe_3O_4) MNPs is 25 nm in diameter and 99.5% purity as stated by the manufacturer (Co., Cairo, Egypt). The tungsten (VI) oxide nanoparticles (WO_3) (purity, 99.5%) had been purchased from Sigma-Aldrich (United States of America). All solutions utilized for the trials have been synthesized from analytical chemicals. Prior to use in the experiments, the reaction containers were washed numerous times with de-ionized water after being cleaned with 10% HNO_3. Phosphate solution (P) of 1000 mg/L was created by dissolving KH_2PO_4 in distilling water. The actual concentration of each solution used was evaluated and diluted as needed based on the necessary doses. The required pH value of the solutions was controlled using a solution of (0.1 M) NaOH and (0.1 M) HCl.

Characterization of nanoparticles

Several techniques can be used to characterize the crystal structure of NPs, such as Scanning Electron Microscopy (SEM), Energy Disperse X-ray (EDX) and Fourier transform infrared spectra (FT-IR). These techniques are employed to ascertain the size, elemental content of surface, shape and crystallinity of NPs.

Batch experiments procedure

It is worth noting that some previous studies have been used, which have set the limits of the variables affecting the processes of removing pollutants using nanoparticles but in this research, the range limits of the variables affecting the effectiveness of P removal from aqueous solutions using nanoparticles have been expanded to determine the best variables that achieve the highest results for the removal. Furthermore, the best ideal variables were used in the case of P removal from real samples of agricultural wastewater by nanoparticles. Therefore, experiments were carried out in 15 mL polypropylene batches, then the concentration of P was adjusted and the adsorbent was added to the aqueous solutions, and after that it was blended in a shaker of water bath to control the temperature. The variables considered in this research; the dosage of adsorbent (0.01–1.5 g/L), the initial P concentrations (5–250 mg/L), retention period (10–1440 minutes), pH (2–13), and temperature (15– 60 °C). The samples were placed into a shaker that rotates at the velocity of 120 rpm; then, those tubes were transferred to the centrifuge that rotates at the velocity of 4000 rpm and this continued for 30 minutes. The remaining P ions were separated and its concentration was measured. All experiments were tested for 3 samples and the average result was considered. Finally, the capacity of adsorption (mg/g) was determined using the Eq. 1:

$$q_e = \frac{(C_o - C_e)\,V}{W} \tag{1}$$

where: C_o – the initial P ions quantity concentration (mg /L);
C_e – the P ions quantity concentration at the equilibrium (mg /L);
V – the volume of solution (L);
W – the weight of adsorbent nanoparticles (g).

In addition, the removal ratio % of P (R%) was calculated using Eq. (2) (Mahdavi et al., 2012).

$$R\ \% = \frac{(C_o - C_e)}{C_o} \times 100 \quad (2)$$

Theoretical basis

Adsorption isotherm studies

Adsorption isotherm is important to clarify the amount of pollutants that were absorbed in the adsorption process. Therefore, the obtained data from experimental results will be analyzed using equations of Langmuir & Freundlich, as they are the most often employed equations (Vinod K. Gupta et al., 2011).

Adsorption kinetics studies

The kinetics study is very important for understanding the adsorption movement of P ions during different time periods on a large time scale, to examining the mechanisms of adsorption such as motility and a chemical reaction, and to understand and to predict how time affects movement in the absorption process. Therefore, to evaluate and interpret the provided data, an appropriate kinematic model is needed. The most popular models used for this are pseudo-first-order & pseudo-second-order models (Örnek et al., 2007).

Adsorption thermodynamics

For evaluating the thermodynamic performance of P adsorption by Fe_3O_4 and WO_3 NPs, thermodynamic coefficients including Gibbs free energy change (ΔG°), enthalpy change (ΔH°), and entropy change (ΔS°) are utilized (Burdzy et al., 2022; Mohammadi et al., 2011).

Statistical analysis

Prior adsorption tests were conducted three times, and the results were averaged for them. The statistical functions of Microsoft Excel were used to perform the necessary computations, such as kinetic models' and isotherms' (R^2) coefficients of determination.

RESULTS AND DISCUSSION

Characterization of the adsorbent

A Scanning Electron Microscopy (SEM) analysis was applied to determine the surface forms

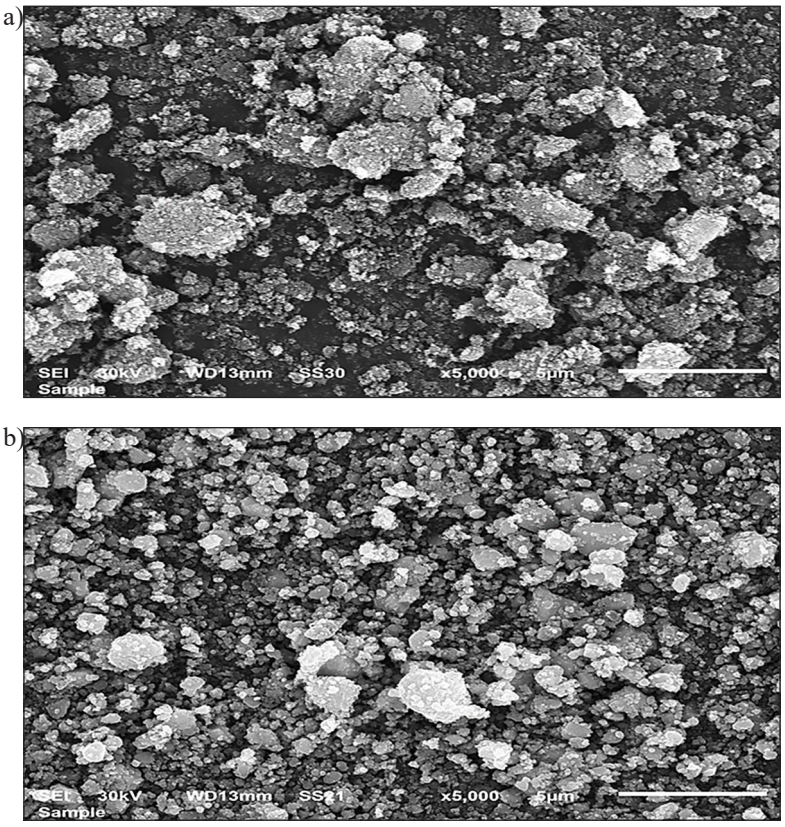

Figure 1. SEM image before adsorption of (a) Fe_3O_4 NP_S (b) WO_3 NP_S

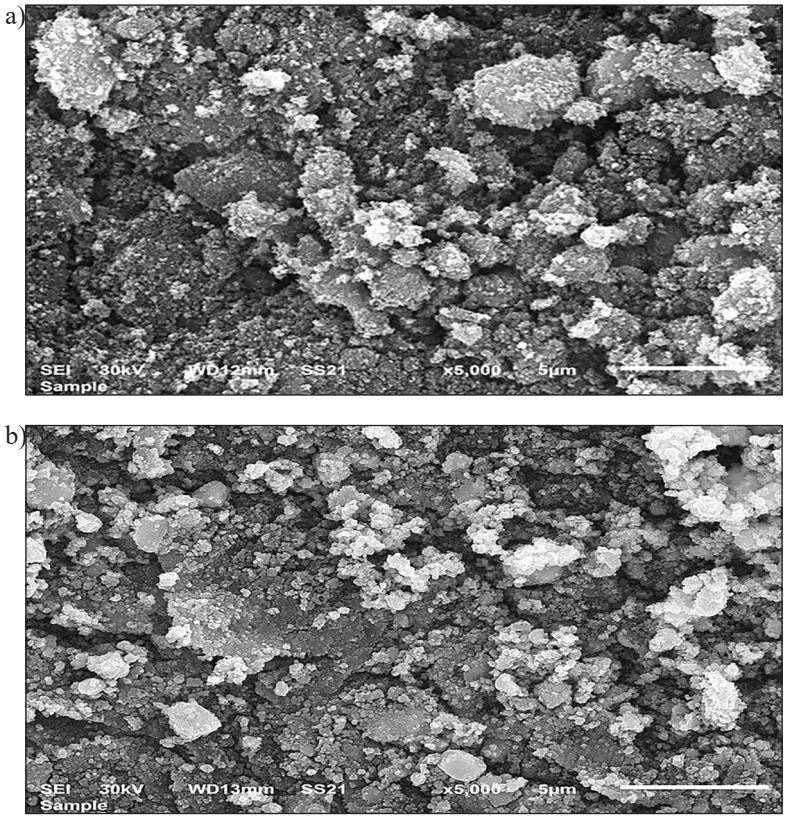

Figure 2. SEM image after adsorption of (a) Fe_3O_4 NP_S (b) WO_3 NP_S

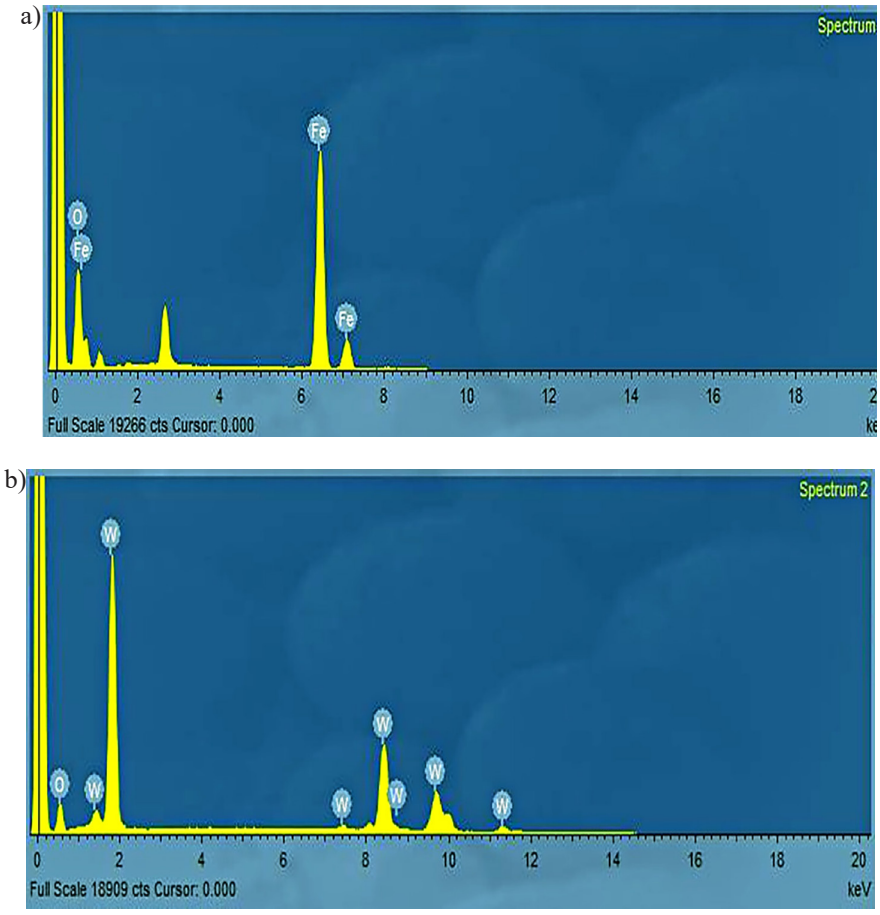

Figure 3. EDX image before adsorption of (a) Fe_3O_4 NP_S (b) WO_3 NP_S

of Fe_3O_4 and WO_3 NPs, SEM images of Fe_3O_4 and WO_3 NPs (magnification power 5,000x) are shown in Figure 1 and Figure 2 before and after absorption respectively. The SEM images after adsorption (Figure 2) showed that the surface of the Fe_3O_4 and WO_3 NPs was heterogeneous, irregular in shape and with a rough surface, but Fe_3O_4 grains were relatively rougher than WO_3 and this explains the high q_e adsorption capacity obtained in the results, where the surface areas of adsorbent materials increase along with surface roughness, which gives more interactions to the adsorption sites (Mahdavi et al., 2014, 2020).

The Energy Disperse X-ray (EDX) measurements are shown in Figure 3 and Figure 4 before and after adsorption, respectively. The EDX measurements of the adsorbents indicate the purity degree on the surfaces of particles. In Figure 3, which shows the state of the adsorbent materials before adsorption, it was concluded that Fe_3O_4 is composed of 75% Iron (Fe) and 25% Oxygen (O) while WO_3 is composed of 90% Tungsten (W) and 10% Oxygen (O), this indicates that there are no impurities in the nanoparticles. Figure 4 confirms the adsorption of P using EDX measurements, since the proportion of P after adsorption was approximately 0.6% and less than 0.2% for Fe_3O_4 and WO_3 respectively, and these conclusions are close to that reported by Chaki et al. (2015) and Mahdavi et al. (2020).

The Fourier transform infrared (FTIR) spectrum of Fe_3O_4 and WO_3 NPs is shown in Figure 5 and Figure 6 before and after absorption, respectively. The absorption peak of Fe_3O_4 NPs was at 3384 cm^{-1} as shown in Figure 6a due to the O-H stretching vibration caused by hydroxyl clusters of water on nanoparticles, and absorption has been repeated several times; it appeared at 3167, 1630, 1479, 1441, 1077, 899, and 799 cm^{-1}, absorption peaks at 636 and 504 cm^{-1} is corresponding to the Fe–O bond Vibration of Fe_3O_4 NPs. The results are close to the values indicated by Chaki et al. (2015) who reported that the absorption peak was between 468.80–695.29 cm^{-1}, corresponding the Fe–O bond vibration. Figure 6b shows the spectrum of WO_3, the peak of absorption at 3449 cm^{-1} is due to the O-H stretching, and absorption has been repeated several times; it appears in the

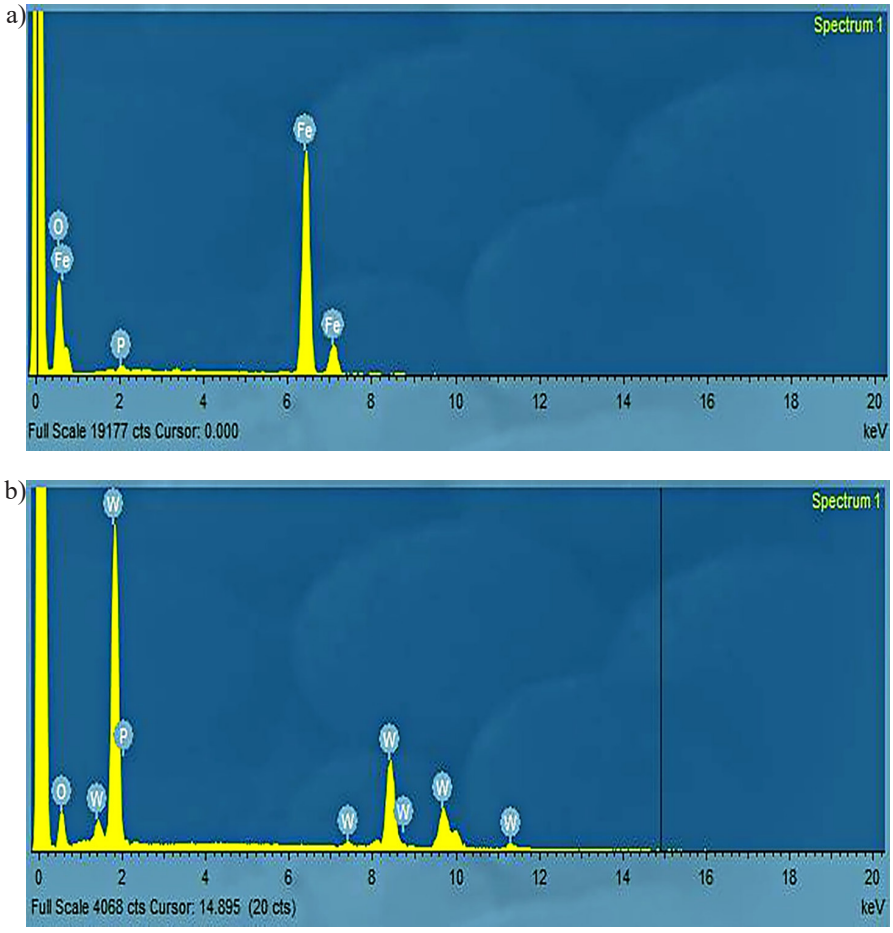

Figure 4. EDX image after adsorption of (a) Fe_3O_4 NP_S (b) WO_3 NP_S

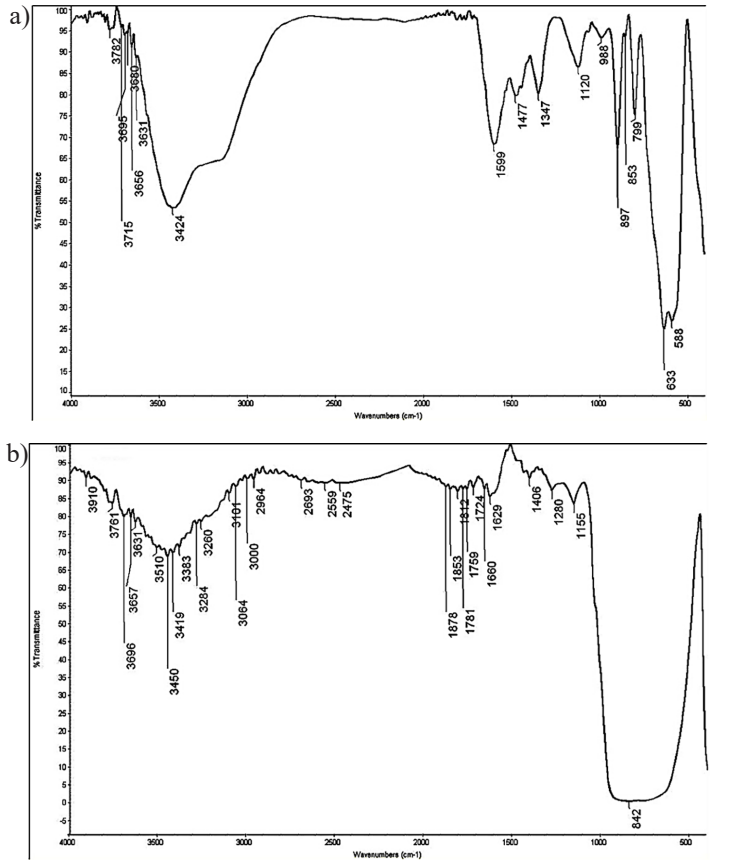

Figure 5. FT-IR image before adsorption of (a) Fe_3O_4 NP_S (b) WO_3 NP_S

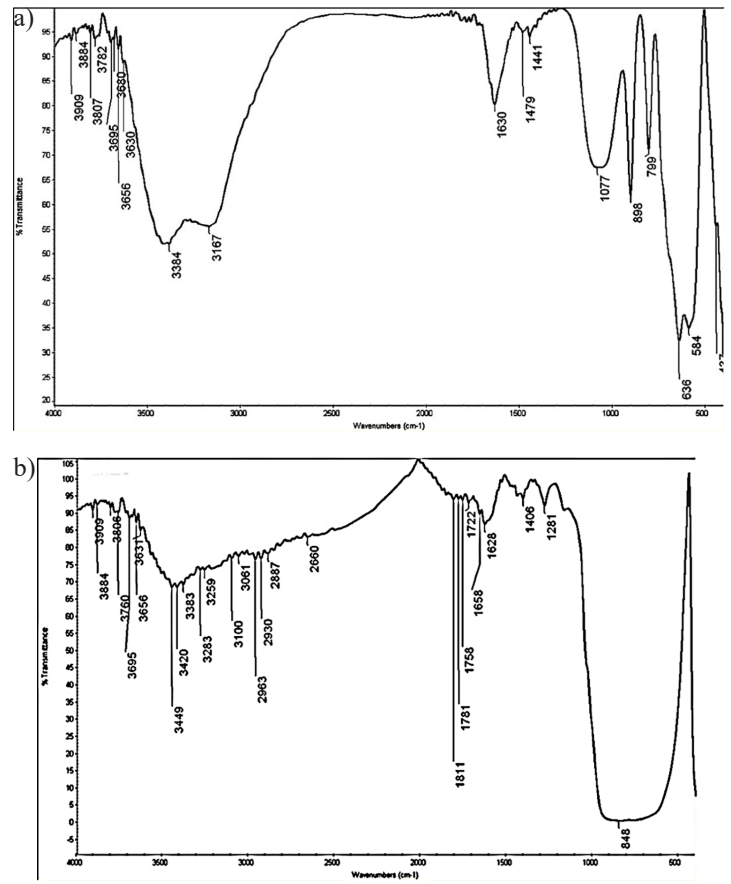

Figure 6. FT-IR image after adsorption of (a) Fe_3O_4 NP_S (b) WO_3 NP_S

range of 3420–2000 cm^{-1} and 1802–1201 cm^{-1}, the largest absorption peaks appeared at 848 cm^{-1} corresponding to the W–O bond vibration of WO_3 NPs. The study results for these peaks were close to the values indicated by Khan et al., (2018) who reported that the largest absorption peak was between 500–900 cm^{-1} corresponding to the W–O bond vibration.

Optimization of process variables

The dosage of adsorbent effect (nanoparticles initial concentration)

To explore Fe_3O_4 and WO_3 NPs dosages impact on P adsorption and to determine the optimal dose of NPs used in the experiment, various doses of nanoparticles were used with range between 0.01 to 1.5 g/L (retention time = 40 minutes, pH= 3.0, initial P concentration= 50 mg/L, temperature= 25 °C, vibration velocity= 120 rpm) were tested. Figure 7 displays the relation between the dose of the adsorbent which is the nanoparticles used, versus the removal ratio of *P*. The findings revealed that once the dosage of adsorbent was raised (from 0.01 to 1) g/l, the ratio of removal has increased from 64.14 to 81.5 % for Fe_3O_4 and from 63.2 to 78.1% for WO_3 NPs. Similarly, q_e increased from 32.52 mg/g to 41.32 mg/g for Fe_3O_4 and from 32.05 mg/g to 39.6 mg/g for WO_3 when dosage of the adsorbent increased from 0.01 to 1 g/l. However, when the adsorbents dose was raised from 1.25 to 1.5 g/L, a relative stability occurred, accompanied by a small decrease in *P* removal from 81.10 to 81.0% for Fe_3O_4 and from 77.80 to 75.75 % for WO_3 NPs. Similarly, q_e decreased from 41.12 to 41.07 mg/g for Fe_3O_4 and from 39.45 to 38.41 mg/g for WO_3. The reason for the decrease in *P* adsorption may be due to the increase of the dose of Fe_3O_4 and WO_3 which increased the agglomeration of the sorbent molecules, then caused shrinkage and reduction of surface area for the active material, leading to lower removal efficiency of P, or due to the interference between the binding sites; therefore, 1.0 g/L was considered the optimal dose for this experiment and this was also in agreement with the experiments of Moharami & Jalali (2014) and Rahmani et al. (2010).

Initial concentration effect of phosphate

Different P initial concentrations (5, 10, 20, 50, 70, 100, 150, 250 mg/L) were used to determine the initial concentration effect of P on its remove ratio (at pH 3.0, the dosage of adsorbent = 1.0 g/L, retention time = 40 minutes, temperature = 25 °C and vibration velocity = 120 rpm). Figure 8 showed that the removal ratio rose as the initial *P* concentration increased, while the uptake of P decreased. When the initial *P* concentration was low (5 mg/L), the *P* removal ratio were 91.64 and 87.14% for Fe_3O_4 and WO_3 NPs respectively and q_e was 5.77 and 5.49 mg/g for Fe_3O_4 and WO_3 NPs respectively. When the initial P concentration were raised to 250 mg/L, the removal ratio was 53.1 and 51.4% for Fe_3O_4 and WO_3 NPs respectively, and q_e was 133.07 and 128.81 mg/g for Fe_3O_4 and WO_3 NPs, respectively. The reason for this may be that when the amount of *P*

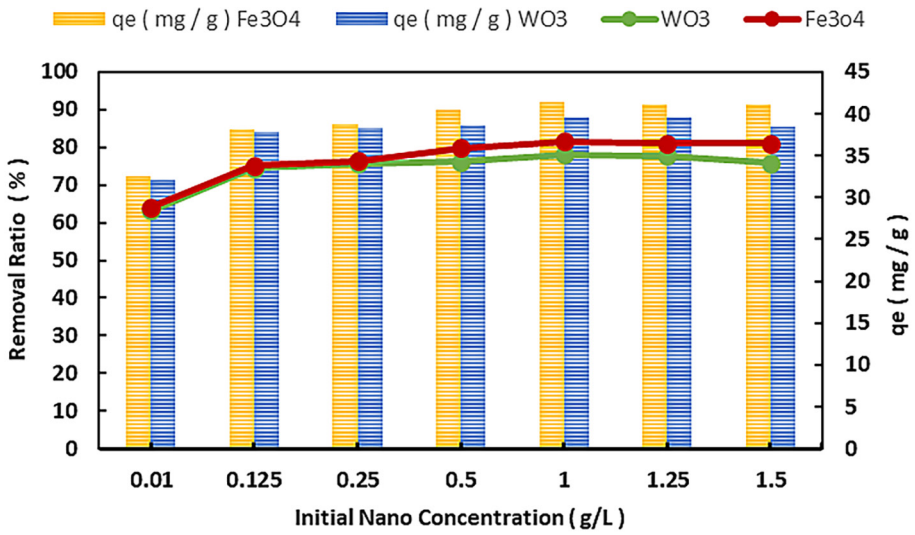

Figure 7. The dosage of adsorbent effect on phosphate removal (initial *P* concentration, 50 mg /L; retention time, 40 min; PH, 3.0; temperature, 25 °C)

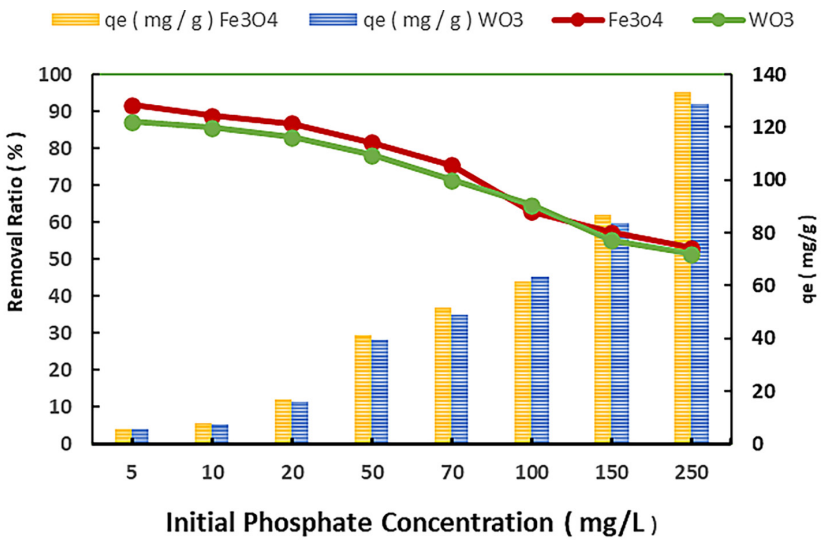

Figure 8. Initial concentration effect of phosphate on phosphate removal (retention time, 40 min; adsorbent dosage, 1.0 g/ L; pH, 3.0; temperature, 25 °C)

concentration increases with the stability of the adsorbent material, the sites of active of the sorbent surface are full of *P* ions until they reach the state of complete saturation. Therefore, the amount of added *P* above the permissible limit exceeded the adsorbent capacity of the sorbent, causing a decrease in *P* ions absorption, so it can be concluded that large concentrations of *P* can be absorbed, but the concentration of adsorbent doses must be increased and this is in agreement with the opinion of Wahab et al. (2011).

Retention time effect

Without a doubt, the process of adsorption depends on time. Figure 9 illustrates the relationship between retention time and removal ratio (at the dosage of adsorbent = 1.0 g/L, pH = 3.0, initial P concentration = 50 mg/L, temperature = 25 °C, vibration velocity = 120 rpm).

In this figure, the adsorption rate of P ions was fast in the first 40 minutes of the experiment. The removal ratio increased from 78.76% at 10 min to 81.5% for at 40 min for Fe_3O_4 NPs and from 74.13% at 10 min to 78.1% at 40 min for WO_3 respectively. Similarly, when retention time was extended from 10 min to 40 min q_e increased from 39.9 to 41.32 mg/g for Fe_3O_4 and from 37.6 to 39.6 mg/g for WO_3. According to Pan et al. (2010) the uptake of P using Fe_3O_4 NPs was extremely rapid and equilibrium was achieved quickly. It was concluded from the results in Figure 9 that the rate of adsorption is extremely

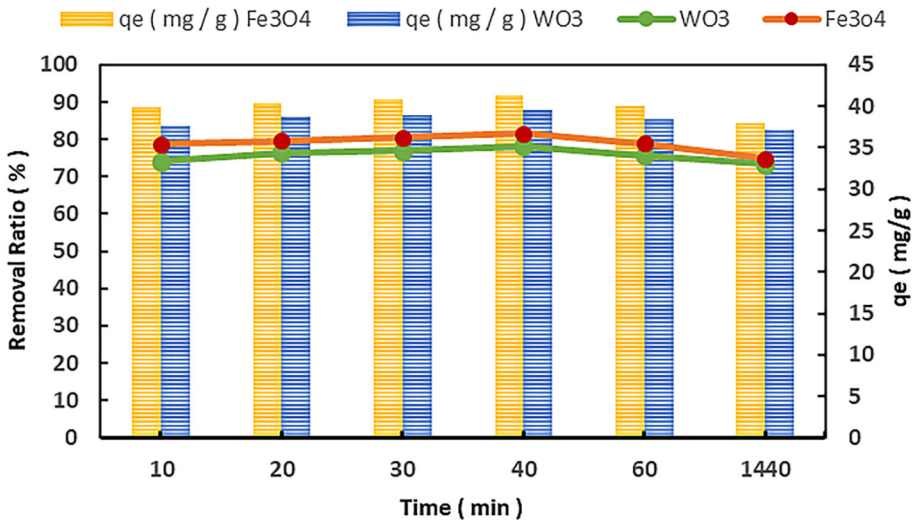

Figure 9. Retention time effect on phosphate removal (initial P concentration, 50 mg/ L; dosage of adsorbent,1.0 g/ L; PH, 3.0; temperature, 25 °C)

rapid for the first 40 minutes of the experiment for both adsorbents (Fe_3O_4 and WO_3 NPs) and then decreases by increasing the contact time, until it reaches the stage of stability. Mustapha et al. (2019) indicated that significantly increased rate of P uptake at the starting of the contact time may be due to the presence of a substantial number of empty adsorption sites ready for the adsorption process, which resulted in a significant increase in the adsorption rate of P; Then, a slight decrease in the adsorption rate occurred with the increase in time, which could be due to the arrival of most of the binding sites to the saturation phase, and as the time continued to increase, the overlap between the binding sites increased; this brought about an increase in the agglomeration of P ions around the surface of the adsorbent particles, and thus the rate of P uptake was decreased. This is in agreement with Edet and Ifelebuegu (2020)

PH effect

The pH is one of the most crucial variables impacting absorption. Adsorption was investigated across a pH range of 2 to 13 in order to identify the ideal pH for maximum removal of P ions (at the dosage of adsorbent= 1.0 g/l, retention time= 40 minutes, initial P concentration= 50 mg/l, temperature 25 °C, vibration velocity= 120 rpm). The results of removing P from aqueous solutions by Fe_3O_4 and WO_3 NPs depending on changes in pH values are shown in Figure 10. It was revealed that the largest absorption of P was at the acidic pH range from 2 to 7; then, absorption decreased when the pH was increased. The maximum obtained P removal ratio was at pH= 2 by 82.05% and 78.88% for Fe_3O_4 and WO_3 NPs, respectively, and the capacity of adsorption q_e of 41.6 mg/g and 40.5 mg/g for Fe_3O_4 and WO_3 NPs, respectively. It was noticed that a significant absorption of P by Fe_3O_4 NPs was achieved at pH range from 2 to 4, where removal ratio values ranged from 82.05 to 80.36% and q_e from 41.6 to 40.75 mg/g, and a significant decrease occurred at pH= 7 to reach the lowest removal value of 65.54% at pH of 13. It was also observed that for WO_3 NPs, a significant absorption of P was achieved at pH range from 2 to 4, where removal ratio ranged from 78.88 to 75.76% and q_e from 40.5 to 38.41 mg/g. There was a slight decrease from 4 to 7, and then a large decrease, starting from pH 10 to 13, where the removal ratio value reached 58.34% at pH=13. The increase in the P removal rate at lower pH levels could be attributed to the fact that a surface of nano adsorbent material contains more active sites and a positive charge. Awual et al. (2011) stated the reason is due to the nature of the reaction at low pH since the surface of the Nano adsorbent material is working as anodes while the negative P ions are working as cathodes (P ions are present in aqueous solutions in the form of HPO_4^{2-} or $H_2PO_4^-$), so an electrostatic interaction occurs between them. Therefore, the removal of P ions can be attributed to electrostatic force or ion exchange (Long et al., 2011). In turn, as the pH rises, the absorption of P ions decreases because when pH rises, the amount of surface hydroxyl reduces, so the negative charge on surface of the nano adsorbents increases, and thus electrostatic

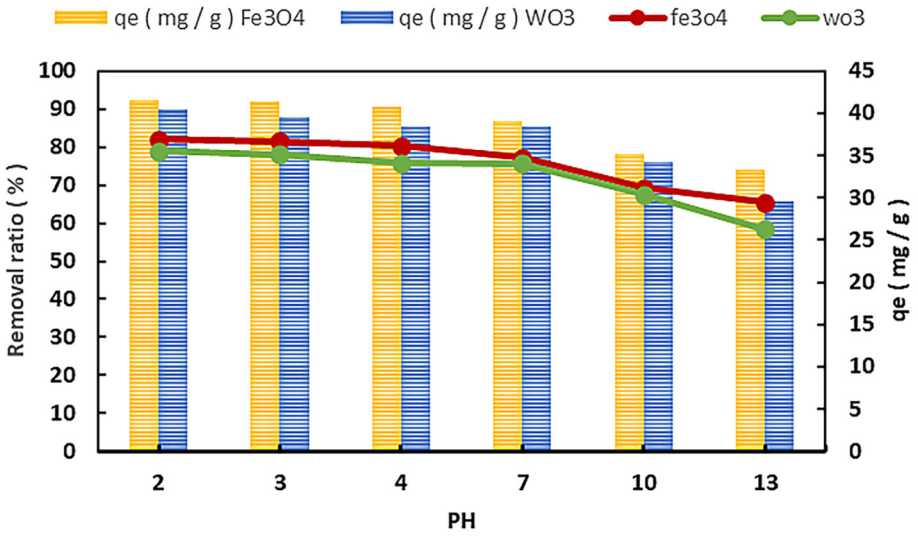

Figure 10. The pH effect on phosphate removal (initial P concentration, 50 mg/ L; dosage of adsorbent, 1.0 g /L; retention time, 40 min; Temperature, 25 °C)

interaction decreases, which leads to a decrease in P absorption, and this is consistent with the opinion of Long et al. (2011).

Temperature effect

Figure 11 illustrated the temperature effects (15 °C, 20 °C, 25 °C, 45 °C, 60 °C) on the removal efficiency of P by Fe_3O_4 and WO_3 NPs (at the dosage of adsorbent = 1.0 g/L, pH= 2.0, retention time= 40 minutes, initial P concentration= 50 mg/L, and vibration velocity= 120 rpm). It was noted that the ability of NPs to absorb P increased along with temperature as that the highest P removal ratio occurred at a temperature of 45 °C, where it was 82.56% and 78.68% for Fe_3O_4 and WO_3 NPs respectively. Results demonstrated that with increasing temperature (from 15 to 45) °C, the ratio of P removed increased from 79.46 to 82.56% and from 71.34 to 78.68% for Fe_3O_4 and WO_3 NPs respectively. Similarly, with increasing temperature (from 15 to 45) °C, q_e rose from 40.29 to 41.86 mg/g for Fe_3O_4 and from 36.17 to 39.89 mg/g for WO_3 which explains that the absorption process is more appropriate at high temperatures. Mustapha et al. (2019) indicated that the reason for the rise in adsorption when the temperature rises can be attributed to the increase in kinetic energy of substance particles at elevated heat, which induces an increase in the collision amplitude between the solute ions and adsorbent particles. When temperature continued to rise from (45 to 60) °C, there was a decrease in the absorption of P, where the removal ratio of P decrease from 82.56 to 80.32% and from 78.68 to 77.48% for Fe_3O_4 and WO_3 NPs, respectively. Similarly, with increasing temperature (from 45 to 60) °C the q_e values decreased from 41.86 to 40.73 mg/g for Fe_3O_4 and from 39.89 to 39.28 mg/g for WO_3. This could be due to the fact that when the temperature increased beyond the required limit, the bonds between the molecules of the adsorbent material and P ions broke down, causing a decrease in the absorption of P ions again. Therefore, it can be considered that the ideal temperature that achieved the highest absorption of P was at 25 to 45 °C, and this outcome is consistent with Mahdavi et al. (2020) and Yoon et al. (2014).

Application of phosphate removal by nanoparticles to agricultural wastewater

This part aimed to apply the nano-treatment technology to a real sample of agricultural wastewater discharged in Diarb Negm drain in Sharkia Governorate, Egypt which contains a large amount of P fertilizers resulting from the agricultural drainage of agricultural lands. Through the experiment, the amount of P in the agricultural drainage water sample mentioned above was measured and it was found that it contains an amount of P of 66 mg/L. The samples were operated under the best operating conditions which achieved the highest amount of adsorption in the experiments that conducted on aqueous solution of P, at (pH = 2.0, retention time = 40 minutes, temperature = 45 °C, adsorbent dose = 1.32 g/L, vibration velocity = 120 rpm), samples were subsequently centrifuged for 30 minutes at 4000 rpm. The removal ratio of P reached 77.3% and 75.42%

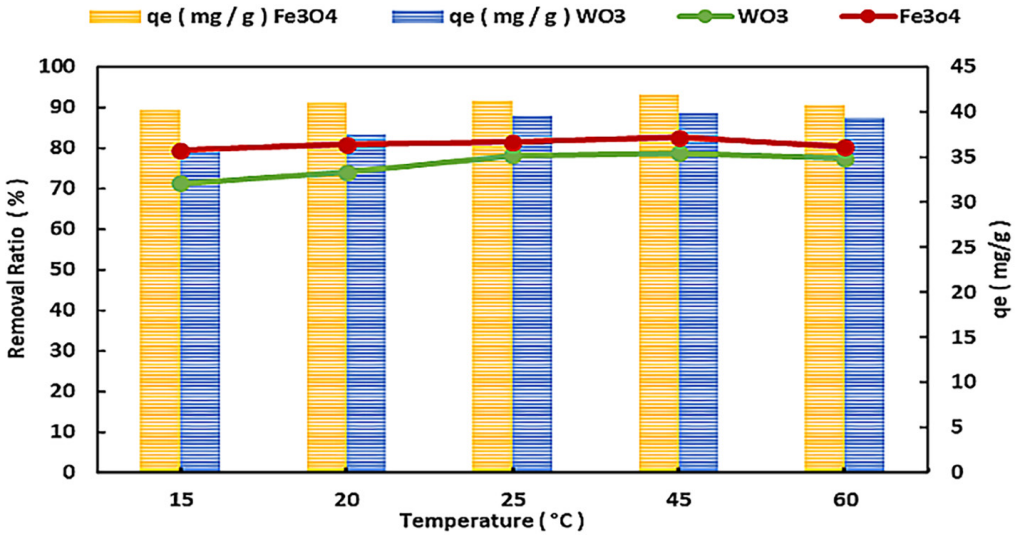

Figure 11. Temperature Effect on phosphate removal (the dosage of adsorbent, 1.0 g/ L; initial P concentration, 50 mg/ L; PH, 2.0; retention time, 40 min)

Table 1. Results of phosphate from the agricultural wastewater (Removal ratio and adsorption capacity) by Fe_3O_4 and WO_3 NPs

The concentration of P in the agricultural wastewater sample 66 mg/L	Fe_3O_4 NPs		WO_3 NPs	
	Removal ratio R (%)	Adsorption capacity q_e (mg/g)	Removal ratio R (%)	Adsorption capacity q_e (mg/g)
	77.3	39.27	75.42	38.31

for Fe_3O_4 and WO_3 NPs respectively, as shown in Table 1. As a result, nanoparticles can be used in treatment of agricultural drainage to remove pollutants, due to the speed of nanoparticles in removing pollutants and their high efficiency.

Theoretical basis

The effect of Adsorption isotherms

The data obtained from equilibrium adsorption were analyzed using the isotherms method to investigate how P ions interact with adsorbents in dynamic balance at fixed temperature. Isotherm studies help in evaluating the distribution of active sites on the surface of the adsorbent material, and provide information regarding the maximum absorption capacity (Gupta et al., 2011), which is useful information for comparison between different adsorbents. Therefore, two different isotherms have been applied, namely Langmuir (Eq. 3) and Freundlich (Eq. 5) models.

The Langmuir equation for isotherms adsorption

The following equation is a representation of the linear function for the Langmuir adsorption isothermal:

$$\frac{C_e}{q_e} = \left[\left(\frac{1}{K_L q_{max}}\right) + \left(\frac{1}{q_{max}}\right) C_e\right] \quad (3)$$

where: q_e – is the quantity of P ions adsorbed per unit weight of the required nanoparticles during a specified equilibrium (mg/g);
C_e – the P ions quantity concentration at the equilibrium (mg /L);
q_{max} – the maximum amount of P ions per unit weight of nanoparticles needed;
K_L – the Langmuir constant linked to the affinity of P ions binding sites (L/mg) (Gupta et al., 2011).

$$R_L = \left(\frac{1}{1+C_o K_L}\right) \quad (4)$$

where: R_L – is a factor called the equilibrium coefficient as specified in the equation.

R_L is applied to indicate whether process if ($0.0 < R_L < 1.0$) is favorable process, if ($R_L > 1$) is unfavorable process, if ($R_L = 1.0$) is linear process, and if ($R_L = 0.0$) is irreversible process (Meroufel et al., 2013).

Langmuir model was used to model the absorption of P ions as mentioned in Table 2. The table describes the coefficients values of Langmuir model for P ions adsorption on Fe_3O_4 and WO_3 NPs. The R_L values is 0.3406 and 0.3417 for Fe_3O_4 and WO_3 NPs so the process is favorable ($0 < R_L < 1$) where the scores tend towards zero (this indicates that absorption is perfect and irreversible) (Meroufel et al., 2013). The q_m values were (0.98, 1.048) mg/g for Fe_3O_4 and WO_3 NPs respectively, and K_L values were about (0.0543, 0.0541) L/mg for Fe_3O_4 and WO_3 NPs respectively. The value of q_m expresses the effectiveness of the adsorption of substances, and it was found that the value of q_m for WO_3 NPs is higher than q_m for Fe_3O_4 NPs, and this is contrary to the results obtained through experiments. Moreover, the linear regression coefficients (R^2) were equal to 0.9374 and 0.9373 for Fe_3O_4 and WO_3 NPs respectively. Therefore, it is considered that the Langmuir model is inappropriate for analyzing the P ions biosorption by Fe_3O_4 and WO_3 NPs.

The Freundlich equation for isotherms adsorption

An experimental model called a Freundlich isotherm displays inhomogeneous adsorption energies at the adsorbent surface (Mittal et al., 2010). Freundlich model means multi-layered and heterogeneous adsorption (Freundlich, H., 1906). Freundlich model assumes several assumptions for the adsorption state, namely:

1. Adsorption can occur in several layers, making it difficult to reach the state of saturation.
2. The Freundlich model is based on the assumption that active sites on the surfaces are strongly heterogeneous.
3. Freundlich's model presupposes that the adsorption process in solutions in the case of heterogeneous surfaces is more responsive.

The Freundlich equation can be expressed in its linear form as:

$$\log q_e = \log K_F + \frac{1}{\mathrm{n}\log C_e} \quad (5)$$

where: q_e – the quantity of P ions adsorbed per unit weight of the required nanoparticles during a specified equilibrium (mg/g);
C_e – the P ions quantity concentration at the equilibrium (mg /L);
K_F – is Freundlich factor indicates the capacity of adsorption (mg /g);
n – constant that symbolizes the strength of adsorption.

Table 2 summarize the Freundlich isotherms coefficients. The coefficient of Freundlich distribution (K_F), and the quantity of energies of the adsorption and desorption can be estimated from the constant (n), and 1/n is a factor of heterogeneity. The adsorption capacity and strength are related to the heterogeneity coefficient 1/n. A lower value of 1/n means that the surface is not homogeneous. The closer 1/n is to zero, the greater the adsorption surface inhomogeneity (Abdo, 2022). If the n value was confined between 1 and 10, then the adsorption capacity is high, where if the n values are less than 1.0, this means that the adsorption capacity is small (Edet & Ifelebuegu, 2020). According to Table 2, Freundlich's K_F values and n values were (8.92, 1.74) and (7.04, 1.61) for Fe_3O_4 and WO_3, NPs respectively. The values of n of Fe_3O_4 and WO_3 NPs were more than 1, which means the adsorption capacity is high. In addition, the Freundlich model's R^2 regression coefficient was 0.9846 and 0.9874 for Fe_3O_4 and WO_3 NPs, respectively, which indicate that Freundlich model is more appropriate and since the R^2 for Freundlich isotherms is more than that of Langmuir, so the Freundlich model outperforms the Langmuir model in terms of data fitting.

The effect of adsorption kinetics

To better comprehend the characteristics of adsorption process with the contact time, pseudo first order and pseudo second order adsorption models were used to obtain the fitting of the experimental data from batch trials. Kinetic parameters for adsorption of phosphate onto nano adsorbent are presented in Table 3.

Pseudo first order equation

The following equation provides a representation of the kinetic model of pseudo first order:

$$\log(q_e - q_t) = \log q_e - \left[\left(\frac{K_1}{2.303}\right)t\right] \quad (6)$$

where: q_e – is the quantity of P ions adsorbed per unit weight of the required nanoparticles during a specified equilibrium (mg/g);
q_t – the quantity of P ions adsorbed per unit weight of the required nanoparticles during a specified time (mg/g);
K_1 – is the pseudo first order adsorption rate constant (min^{-1}) (Simonin, 2016);
t – is the contact time of tests (hr).

Table 3 shows that the pseudo first order model's correlation coefficients (R^2) were low, since its value was equal to 0.6776 and 0.423 for Fe_3O_4 and WO_3 respectively. Therefore, this model is not suitable and not compatible to express the kinetic model of the experimental data.

Pseudo-second-order equation

The following equation provides a representation of the kinetic model of pseudo second order:

$$\frac{\mathrm{t}}{q_t} = \left(\frac{1}{K_2 * q_e^2}\right) + \frac{t}{q_e} \quad (7)$$

where: q_e – the quantity of P ions adsorbed per unit weight of the required nanoparticles at equilibrium of specified (mg/g);
K_2 – is the pseudo second order rate constant of adsorption (g/mg/min) (Ho & McKay, 1999);
t – the contact time of the experiments (hr).

Table 3 displays the parameters and correlation coefficients for pseudo second order. According to the R^2 correlation coefficients, the second-order model fits experimental data more strongly

Table 2. The isothermal parameters for phosphate adsorption by the nanoparticle's adsorbent

Adsorption isothermal	Langmuir isothermal model			Freundlich isothermal model		
NPs adsorbent	R^2	(mg/g)	(L/mg)	R^2	n	(mg/g)
Fe_3O_4 NPs	0.9374	0.98	0.0543	0.9846	1.745	8.92
WO_3 NPs	0.9373	1.048	0.0541	0.9874	1.6129	7.04

Table 3. The kinetic parameters for phosphate adsorption by the nanoparticle's adsorbent

Models of Kinetic	Pseudo first model			Pseudo second model		
NPs adsorbent	R^2	q_e (mg/g)	K_1 (min^{-1})	R^2	q_e (mg/g)	K_2 (g /mg/min)
Fe_3O_4 NPs	0.6776	0.962	-0.0525	0.999	37.87	-0.7679
WO_3 NPs	0.423	1.0509	-0.0345	0.999	37.146	-1.2118

than first order model, as it was found that the correlation coefficient of the studied data is very high ($R^2 > 0.99$). The calculated q_e value from pseudo second order was nearby to the experimental q_e value, since the calculate q_e value was 37.87 and 37.14 mg/g for Fe_3O_4 and WO_3 NPs respectively, while the experimental values of q_e was 41.32 and 39.6 mg/g for Fe_3O_4 and WO_3 NPs, respectively, which confirms that pseudo second order model matching *P* ions adsorption using the nanoparticles (Upadhyay et al., 2021). Similar results were reported by Long et al. (2011) who indicated that pseudo-second-order kinetics are the ones that better represent *P* uptake. Since the absorption of *P* fits the pseudo second order kinetic model, this suggests that rate-determining stage of process is the chemical adsorption among *P* and active sites of the adsorbent. In accordance with the test results, it was concluded that the adsorption occurred mainly during the first hour of operation, then there was a decrease in absorption after that time.

Adsorption thermodynamics analysis

The evaluation of the thermodynamic performance of *P* adsorption by Fe_3O_4 and WO_3 NPs was completed using the thermodynamic analysis, where the thermodynamic response to adsorption of *P* from nanoparticles was evaluated using the parameters Gibbs free energy change (ΔG°), enthalpy change (Δ*H*°), and entropy change (Δ*S*°) (Katarzyna Burdzy et al., 2022; Mohammadi et al., 2011).

$$\Delta G^{o} = -R\,T\,LnK_d \tag{8}$$

$$K_d = \frac{q_e}{Ce} \tag{9}$$

$$\mathrm{Ln}\,K_d = \frac{\Delta S^o}{R} - \frac{\Delta H^o}{R\,T} \tag{10}$$

where: T – is the temperature of the experiments (Kelvin K);
K_d – represents the temperature equilibrium constant;
R – ideal gas constant, which is equal to (8.314 J mol^{-1}K^{-1});
q_e – the quantity of *P* ions adsorbed per unit weight of the required nanoparticles during a specified equilibrium (mg/g);
C_e – the *P* ions quantity concentration at the equilibrium (mg /L).

According to the results of thermodynamic equations, thermodynamic coefficients like (Δ*G*°, Δ*H*° and Δ*S*°) are of great importance when evaluating the practicality of thermodynamic and the adsorption mechanism character. Table 4 displays the simulated results for the thermodynamic coefficients. Negative values of Δ*G*° acquired in the analysis indicate that the P ions adsorption by Fe_3O_4 and WO_3 NPs is spontaneous and favorably of thermodynamic at all examined temperatures. Moreover, the values of Δ*G*° progressively increase as the temperature rises, which indicates that increase in temperature has enhanced the

Table 4. The parameters of thermodynamic for phosphate adsorption by the nanoparticle's adsorbent

NPs adsorbent	Temp	Ln K_d	Δ*G*° (KJ.)	Δ*H*° (KJ.)	Δ*S*° (J.)
Fe_3O_4 NPs	15	+1.353	-3.24047	+ 1.0619	+ 15.5171
	20	+1.440	-3.50826		
	25	+1.482	-3.67366		
	45	+1.555	-4.11130		
	60	+1.4073	-3.89643		
WO_3 NPs	15	+0.9120	-2.18375	+ 5.0749	+ 26.23208
	20	+1.04719	-2.55097		
	25	+1.2718	-3.15118		
	45	+1.3056	-3.4529		
	60	+1.2353	-3.42014		

ability to adsorb *P* ions by nanoparticles, which means that higher temperature is more suitable for the process of adsorption. This was also indicated by Liu & Hu (2019), as they stated that when the temperature increases, the kinetic energy of the particles rises, this causes a rise in collision amplitude between the adsorbent material and P ions. The heat coefficients ($\Delta H°$) for Fe_3O_4 and WO_3 NPs were positive (+1.0619 and +5.0749), respectively. Positive values of $\Delta H°$ indicate that reaction is endothermic in the two processes. In turn, positive values of $\Delta S°$ for Fe_3O_4 and WO_3 NPs (+15.5171 and +26.232), respectively, confirm random increase in the reaction during the adsorption process. This is what is indicated by Katarzyna Burdzy et al. (2022).

CONCLUSION

Water quality is a major factor for the general health of humans, living organisms and aquatic life. By 2025, two-thirds of the world's population could face water deficiency and that it worth noting that Egypt is one of the countries facing the threats of water scarcity due to the continuous increase in the population with limited water resources. Therefore, water quality assessment and treatment has become a global issue of human interest. It was necessary to highlight many issues of surface water purification, as well as the reuse of wastewater and its treatment of pollutants in effective and low-cost ways. Phosphate (P) is one of the pollutants that negatively affect the quality of water and the living organisms in it. Therefore, the present work has been undertaken with the objective of exploring mechanism for using Fe_3O_4 and WO_3 NPs as effective adsorbents to remove and dispose of P ions from agricultural wastewater. Adsorption of P using the aforementioned nanoparticles was studied in laboratory experiments using aqueous solutions of phosphate at contact time from 10–1440 min, at values of pH from 2–13 and at temperature from 15–60 °C. The analyses of the results indicated that after chemical treatments, the P ions were absorbed efficiently from the water using Fe_3O_4 and WO_3 NPs nanomaterials. The best removal rate was achieved at 40 min, 2.0 pH and 45 °C. The best ideal variants were applied to real samples of agricultural wastewater and the removal ratio of *P* reached 77.3% and 75.42% for Fe_3O_4 and WO_3 NPs respectively. In addition, the results of laboratory experiments of adsorption of P from aqueous solutions of phosphate using the aforementioned nanoparticles were analyzed using pseudo first order & pseudo second order equations for examining adsorption kinetics. The findings indicate that the pseudo second order fits better than pseudo first order since q_e values computed from pseudo second order was nearby to the experimental q_e value and the R^2 correlation coefficient for pseudo second order was greater than R^2 value for pseudo first order. In addition, Langmuir & Freundlich theories were applied to describe *P* adsorption isotherms. These equilibrium data showed that Freundlich model is more suitable to represent results than the Langmuir model. In addition, the data were analyzed by thermodynamic equations and it was found that the process of P ions adsorption by Fe_3O_4 and WO_3 NPs is spontaneous, random and endothermic. Further researches are needed for studying the adsorption efficiency of WO_3 NPs for other pollutants.

REFERENCES

1. Abdo, A. 2022. Potentiality of unfertilized mango flowering buds for removing Cd, Cu, and Pb from aqueous solutions. Desalination and Water Treatment, 247, 144–155. https://doi.org/10.5004/dwt.2022.28038
2. Abiodun Segun, A., Morufu Olalekan, R. 2021. When Water Turns Deadly: Investigating Source Identification and Quality of Drinking Water in Piwoyi Community of Federal Capital Territory, Abuja Nigeria. Trends Journal of Sciences Research, 1(1), 38–58. https://doi.org/10.31586/ojc.2021.010105
3. Adeleye, A.S., Conway, J.R., Garner, K., Huang, Y., Su, Y., Keller, A.A. 2016. Engineered nanomaterials for water treatment and remediation: Costs, benefits, and applicability. Chemical Engineering Journal, 286, 640–662. https://doi.org/10.1016/j.cej.2015.10.105
4. Awual, M.R., Jyo, A., El-Safty, S.A., Tamada, M., Seko, N. 2011. A weak-base fibrous anion exchanger effective for rapid phosphate removal from water. Journal of Hazardous Materials. https://doi.org/10.1016/j.jhazmat.2011.01.092
5. Chaki, S.H., Malek, T.J., Chaudhary, M.D., Tailor, J.P., Deshpande, M.P. 2015. Magnetite Fe3O4 nanoparticles synthesis by wet chemical reduction and their characterization. Advances in Natural Sciences: Nanoscience and Nanotechnology, 6(3), 1–6. https://doi.org/10.1088/2043-6262/6/3/035009

6. Chen, L., Zhao, X., Pan, B., Zhang, W., Hua, M., Lv, L., Zhang, W. 2015. Preferable removal of phosphate from water using hydrous zirconium oxide-based nanocomposite of high stability. Journal of Hazardous Materials. https://doi.org/10.1016/j.jhazmat.2014.10.048
7. Chen, N., Feng, C., Yang, J., Gao, Y., Li, M., Zhang, B. 2013. Preparation and characterization of ferric-impregnated granular ceramics (FGCs) for phosphorus removal from aqueous solution. Clean Technologies and Environmental Policy. https://doi.org/10.1007/s10098-012-0527-9
8. Edet, U.A., Ifelebuegu, A.O. 2020. Kinetics, isotherms, and thermodynamic modeling of the adsorption of phosphates from model wastewater using recycled brick waste. Processes, 8(6). https://doi.org/10.3390/PR8060665
9. Freundlich, H. 1906. Adsorption in solution. Phys. Chem, 40, 1361–1368.
10. Gomaah, M., Ramadan, A., El-Shazly, M.M., Abdulhady, Y.A., Shawky, H.A. 2021. Physicochemical and Bacteriological Quality of Groundwater, East of Nile Delta of Egypt. Journal of Geoscience and Environment Protection, 9.
11. Gupta, V.K., Jain, R., Nayak, A., Agarwal, S., Shrivastava, M. 2011. Removal of the hazardous dye-Tartrazine by photodegradation on titanium dioxide surface. Materials Science and Engineering C. https://doi.org/10.1016/j.msec.2011.03.006
12. Ho, Y.S., McKay, G. 1999. Pseudo-second order model for sorption processes. Process Biochemistry. https://doi.org/10.1016/S0032-9592(98)00112-5
13. Burdzy, K., Chen, Y.-G., Lv, G.-Y., Chen, S.-H., Kołodyńska, D. 2022. Application of Ion Exchangers with the N-Methyl-D-Glucamine Groups in the V(V) Ions Adsorption Process. Materials, 15(3).
14. Khan, M.A.M., Kumar, S., Ahamad, T., Alhazaa, A.N. 2018. Enhancement of photocatalytic and electrochemical properties of hydrothermally synthesized WO3 nanoparticles via Ag loading. Journal of Alloys and Compounds, 743, 485–493. https://doi.org/10.1016/j.jallcom.2018.01.343
15. Khodadadi, M., Hosseinnejad, A., Rafati, L., Dorri, H., Nasseh, N. 2017. Removal of Phosphate from Aqueous Solutions by Iron Nano-Magnetic Particle Coated with Powder Activated Carbon TT -. Bums-Hstj.
16. Leduc, J.F., Leduc, R., Cabana, H. 2014. Phosphate adsorption onto chitosan-based hydrogel microspheres. Adsorption Science and Technology. https://doi.org/10.1260/0263-6174.32.7.557
17. Liu, Y., Hu, X. 2019. Kinetics and thermodynamics of efficient phosphorus removal by a composite fiber. Applied Sciences (Switzerland). https://doi.org/10.3390/app9112220
18. Long, F., Gong, J.L., Zeng, G.M., Chen, L., Wang, X.Y., Deng, J.H., Niu, Q.Y., Zhang, H.Y., Zhang, X.R. 2011. Removal of phosphate from aqueous solution by magnetic Fe-Zr binary oxide. Chemical Engineering Journal. https://doi.org/10.1016/j.cej.2011.03.102
19. Mahdavi, S., Hassani, A., Merrikhpour, H. 2020. Aqueous phosphorous adsorption onto SnO2 and WO3 nanoparticles in batch mode: kinetic, isotherm and thermodynamic study. Journal of Experimental Nanoscience. https://doi.org/10.1080/17458080.2020.1770733
20. Mahdavi, S., Jalali, M., Afkhami, A. 2014. Removal of heavy metals from aqueous solutions using Fe3O4, ZnO, and CuO nanoparticles. In Nanotechnology for Sustainable Development, First Edition. https://doi.org/10.1007/978-3-319-05041-6_14
21. Meroufel, B., Benali, O., Benyahia, M., Benmoussa, Y., Zenasni, M.A. 2013. Adsorptive removal of anionic dye from aqueous solutions by Algerian kaolin: Characteristics, isotherm, kinetic and thermodynamic studies. Journal of Materials and Environmental Science, 4(3), 482–491.
22. Mishra, S.P., Das, M., Dash, U.N. 2010. Review on adverse effects of water contaminants like arsenic, fluoride and phosphate and their remediation. In Journal of Scientific and Industrial Research.
23. Mittal, A., Mittal, J., Malviya, A., Gupta, V.K. 2010. Removal and recovery of Chrysoidine Y from aqueous solutions by waste materials. Journal of Colloid and Interface Science. https://doi.org/10.1016/j.jcis.2010.01.007
24. Mohammadi, N., Khani, H., Gupta, V.K., Amereh, E., Agarwal, S. 2011. Adsorption process of methyl orange dye onto mesoporous carbon material-kinetic and thermodynamic studies. Journal of Colloid and Interface Science. https://doi.org/10.1016/j.jcis.2011.06.067
25. Moharami, S., Jalali, M. 2014. Effect of TiO2, Al2O3, and Fe3O4 nanoparticles on phosphorus removal from aqueous solution. Environmental Progress and Sustainable Energy. https://doi.org/10.1002/ep.11917
26. Mustapha, S., Shuaib, D.T., Ndamitso, M.M., Etsuyankpa, M.B., Sumaila, A., Mohammed, U.M., Nasirudeen, M.B. 2019. Adsorption isotherm, kinetic and thermodynamic studies for the removal of Pb(II), Cd(II), Zn(II) and Cu(II) ions from aqueous solutions using Albizia lebbeck pods. Applied Water Science, 9(6). https://doi.org/10.1007/s13201-019-1021-x
27. Örnek, A., Özacar, M., Şengil, I.A. 2007. Adsorption of lead onto formaldehyde or sulphuric acid treated acorn waste: Equilibrium and kinetic studies. Biochemical Engineering Journal. https://doi.org/10.1016/j.bej.2007.04.011
28. Pan, G., Li, L., Zhao, D., Chen, H. 2010. Immobilization of non-point phosphorus using stabilized

magnetite nanoparticles with enhanced transportability and reactivity in soils. Environmental Pollution. https://doi.org/10.1016/j.envpol.2009.08.003

29. Panneerselvam, P., Morad, N., Tan, K.A. 2011. Magnetic nanoparticle (F3O4) impregnated onto tea waste for the removal of nickel(II) from aqueous solution. Journal of Hazardous Materials. https://doi.org/10.1016/j.jhazmat.2010.10.102
30. Pica, M. 2021. Treatment of wastewaters with zirconium phosphate based materials: A review on efficient systems for the removal of heavy metal and dye water pollutants. Molecules, 26(8). https://doi.org/10.3390/molecules26082392
31. Rahmani, A., Mousavi, H.Z., Fazli, M. 2010. Effect of nanostructure alumina on adsorption of heavy metals. Desalination. https://doi.org/10.1016/j.desal.2009.11.027
32. Simonin, J.P. 2016. On the comparison of pseudo-first order and pseudo-second order rate laws in the modeling of adsorption kinetics. Chemical Engineering Journal. https://doi.org/10.1016/j.cej.2016.04.079
33. Singh, S.A., Madras, G. 2013. Photocatalytic degradation with combustion synthesized WO3 and WO3TiO2 mixed oxides under UV and visible light. Separation and Purification Technology. https://doi.org/10.1016/j.seppur.2012.12.010
34. Suhas, Gupta, V.K., Carrott, P.J.M., Singh, R., Chaudhary, M., Kushwaha, S. 2016. Cellulose: A review as natural, modified and activated carbon adsorbent. In Bioresource Technology. https://doi.org/10.1016/j.biortech.2016.05.106
35. Taha, A., El-Mahmoudi, A., El-Haddad, I. 2004. Pollution sources and related environmental impacts in the new communities southeast Nile Delta, Egypt. Emirates Journal for Engineering Research, 9(1), 35–49.
36. Upadhyay, U., Sreedhar, I., Singh, S.A., Patel, C.M., Anitha, K.L. 2021. Recent advances in heavy metal removal by chitosan based adsorbents. Carbohydrate Polymers, 251(May 2020), 117000. https://doi.org/10.1016/j.carbpol.2020.117000
37. Wahab, M.A., Hassine, R.B., Jellali, S. 2011. Posidonia oceanica (L.) fibers as a potential low-cost adsorbent for the removal and recovery of orthophosphate. Journal of Hazardous Materials. https://doi.org/10.1016/j.jhazmat.2011.04.085
38. Yoon, S.Y., Lee, C.G., Park, J.A., Kim, J.H., Kim, S.B., Lee, S.H., Choi, J.W. 2014. Kinetic, equilibrium and thermodynamic studies for phosphate adsorption to magnetic iron oxide nanoparticles. Chemical Engineering Journal, 236, 341–347. https://doi.org/10.1016/j.cej.2013.09.053